Available online at www.sciencedirect.com
ScienceDirect
Thin Solid Films 516 (2008) 5523–5526
www.elsevier.com/locate/tsf

Morphology and optoelectronic properties of ZnO rod array/conjugated polymer hybrid films

Chi-Jung Chang [a,*], Mei-Hui Tsai [b], Yu-Hsiang Hsu [a], Chi-Shen Tuan [c]

[a] Department of Chemical Engineering, Feng Chia University, 100, Wenhwa Road, Seatwen, Taichung, 40724, Taiwan, ROC
[b] Department of Chemical and Materials Engineering National Chin-Yi University of Technology, Taichung 411, Taiwan, ROC
[c] Applied Chemistry Division, Union Chemical Laboratories, Industrial Technology Research Institute, Hsinchu, Taiwan, ROC

Available online 14 July 2007

Abstract

Vertically aligned zinc oxide (ZnO) nanorods were grown on the ITO glass and then coated with the conjugated polymer poly(2,3-dibutoxy-1,4-phenylene vinylene) (DB-PPV) to make the hybrid films. Nanorods with different diameters were synthesized to study the influences of ZnO nanorod morphology and polymer infiltration on the photocurrent and optical properties of the hybrid films. Increasing the growth time leads to the formation of ZnO rod array with large rod diameter, large surface area and small inter-rod distance. Small inter-rod distance hinders the filling of DB-PPV into the porous ZnO rod microstructure and lowers the PN junction area. It leads to lower photocurrent of the hybrid film. The red shift of the photoluminescence spectra suggests that filling the polymer into the ZnO rod microstructure favors more planar molecular orientations of the conjugated polymers and leads to an increase in the effective conjugation length.

Keywords: ZnO; Aligned nanorod array; Conjugated polymer; Photocurrent; Photoluminescence

1. Introduction

Recently, it has been shown that composite materials containing the nanostructured electron accepting component and the electron-donating organic semiconductor in a "bulk heterojunction" structure are promising materials for photovoltaic device [1]. Ultra-fast photoinduced charge transfer occurs between the conjugated polymers and the metal oxide semiconductor such as TiO_2, or ZnO [2].

However, the overall performance of such devices is still disappointing because of limited charge transport and charge separation efficiency. Zinc oxide (ZnO) is of interest because of its availability of low temperature synthesis, the high electron mobility, and the potential for preparing the ordered nanostructure by the solution process. Solution synthesis offers the potential for much lower cost because it eliminates the expenses associated with high temperature and vacuum processing. Besides, solution processing is compatible with roll-to-roll processing of flexible plastic substrates. ZnO nanorods grown perpendicular to the substrate are particularly interesting. Perpendicularly oriented single-crystalline ZnO nanorod arrays have been recently fabricated on sapphire substrates using VLS [3] and CVD methods [4]. These methods involve complex procedures, sophisticated equipment and high temperature. Recently, O'Brien et al.[5] and Vayssieres [6] reported the low temperature growth of ZnO nanocolumns from aqueous solution. Vertically aligned ZnO nanorods were used to increase the efficiencies of these photovoltaic devices [7,8]. The ordered zinc oxide nanorods acted as electron acceptors and provided the direct path for photogenerated electrons to the collecting electrode. If the electrons diffuse through the film faster than they recombine, the majority of the charge injected into the semiconductor is collected at the transparent conducting electrode. Devices were prepared by infiltrating conjugated polymers into a mesoporous, nanostructured oxide semiconductor network [9].

Increasing the growth time leads to the formation of ZnO rod array with large rod diameter, high surface area and small inter-rod distances. The distances between the rods influenced the difficulty of filling the mesoporous structure with polymer. No effort has been made on the influences of ZnO nanorod array

* Corresponding author. Tel.: +886 4 24517250x3678; fax: +886 4 24510890.
E-mail address: changcj@fcu.edu.tw (C.-J. Chang).

0040-6090/$ - see front matter © 2007 Elsevier B.V. All rights reserved.
doi:10.1016/j.tsf.2007.07.078

structure on the infiltration of conjugated polymer into a mesoporous ZnO rod array and the photocurrent response. In this paper, ZnO nanorods with different average diameters were synthesized by changing the rod growth time. The influences of rod diameter and inter-rod distance on the morphology and the in-situ photocurrent response of vertically aligned ZnO nanorod-DB-PPV polymer hybrid films were studied.

2. Experimental

Perpendicularly oriented single crystalline ZnO nanorods were grown on ITO substrates by the hydrothermal growth method. The procedure consists of two steps: (1) formation of ZnO nanoparticles as seed on ITO glass substrates, and (2) hydrothermal growth of ZnO nanorods in aqueous solution.

At first, 0.01 M zinc acetate [$Zn(CH_3COO)_2{\cdot}2H_2O$] was dissolved in the ethanol. The solution was cooled to 0 °C. Then, CTAOH (cetyltrimethylammonium hydroxide) was added and the solution was stirred for 30 min. The resulting mixture was then agitated at 60 °C for 2 h to yield a homogeneous and stable colloid solution, which served as the coating solution. After being coated with the colloid solution, the substrates were dried and annealed at 300 °C for 1 h. The ZnO nanorod array was grown at 95 °C in a sealed bottle by immersing the modified substrates in the aqueous solution containing $Zn(NO_3)_2$ (0.05 M) and methenamine (0.05 M). ZnO12 and ZnO14 films mean the rod growth time are 2 and 4 h respectively. DB-PPV was dissolved in THF and spin-coated onto the ZnO rod array at 700 rpm for 10 s. DBZ12 and DBZ14 films represent the DB-PPV/ZnO12 and DB-PPV/ZnO14 hybrid films respectively.

XRD studies were carried out with a MAC SCIENCE MXP3 diffractometer. The morphology of the nanorods was characterized using scanning electron microscopy using a HITACHI S-4800 Field Emission Scanning Electron Microscope (FESEM). The photoluminescence spectra were measured by the PL2006 Multifunction Fluorescent Spectrometer (Labguide co.)

3. Results and discussion

The crystal structure of the nanorod was examined by XRD. Fig. 1 shows an XRD pattern of the ZnO12 nanorod array. The sharp shape of the (0 0 2) diffraction peak suggests that ZnO samples are well crystallized. The remarkably enhanced (0 0 2) diffraction peak is much more intensive than the other peaks, implying that these nanorods were perfectly oriented perpendicular to the substrate surface and that they were grown along the *c*-axis.

The morphology of ZnO nanorods was characterized by FESEM. Fig. 2(a) and (b) show top-view images of the ZnO12 and ZnO14 nanorods respectively. All nanorods were grown in a direction perpendicular to the substrate. Vertically aligned arrays of ZnO nanorods were uniformly grown on the ZnO12 sample with the diameters varying from 25 to 50 nm. The diameter of the ZnO rod on the ZnO14 sample altered from 65 to 165 nm. Increasing the rod growth time widened the rod diameter. There are some closely packed rods that the inter-rod

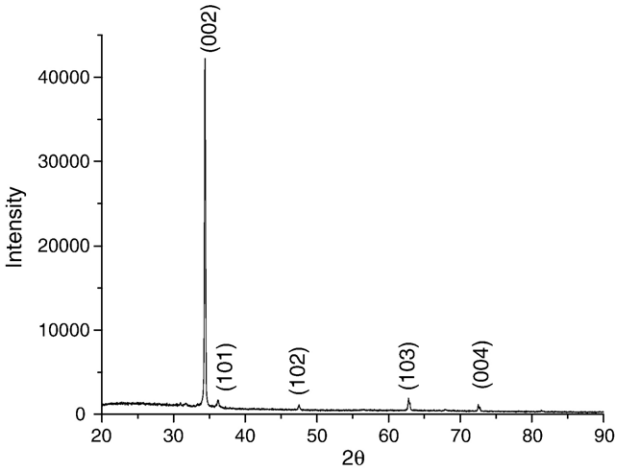

Fig. 1. XRD of ZnO12 nanorods.

distance is close to zero. Although the aspect ratio of the longest nanowires continues to increase with increasing growth time, the number density of nanorods decreases. Some nanorods have stopped growing. Similar phenomena were also observed by Miyashita et al. [10] in the ZnO nanorods prepared by the CVD method. They reported a 'collision' between two non-parallel ZnO nanorods during the growing process. When a nanorod collides with the side of another nanorod, the growth of the colliding nanorod is stopped there. On the other hand, the growth of a nanorod being collided on its side continued after the 'collision'. It is the reason why the number density of nanorods decreases and why the vertical orientation of nanorods is improved after longer growth time.

The DBZ14 film with larger ZnO rod should have larger ZnO surface area than the DBZ12 film did. If the ZnO surface is completely covered by DB-PPV, there will be more donor-acceptor interface area (P–N junction) for the DBZ14 film. More incident photons are absorbed. Because of efficient dissociation of generated excitons and subsequent transport of charge carriers, photocurrent should increase with increasing surface area. To check the coverage of DB-PPV polymer on the ZnO rod, the cross-sectional images of both films were observed by FESEM. Fig. 2(c) showed the cross-sectional FESEM image of DB-PPV polymer infiltrated into the DBZ12 nanorod array structure. The polymer can be effectively intercalated into the ZnO rods film to make a nanostructured oxide/conjugated polymer composite device. The thickness of the hybrid film is about 500 nm. Fig. 2(d) showed the cross-sectional FESEM image of DBZ14 hybrid film. There were some ZnO nanorods that were not covered by the DB-PPV polymer. The closely packed rods with almost zero inter-rod distance (shown in Fig. 2 (b)) hindered the infiltration of polymer into the nanorod array. The thickness of the hybrid film is about 1 μm.

For the conjugated polymers, electron transport can be viewed as a series of hops between shallow trap sites, with a fraction of the sites acting as recombination centers. The use of single crystal nanorods may allow electron transport via extended states in the conduction band, rather than by a series of hops between trap states. In this study, the ZnO rod diameter

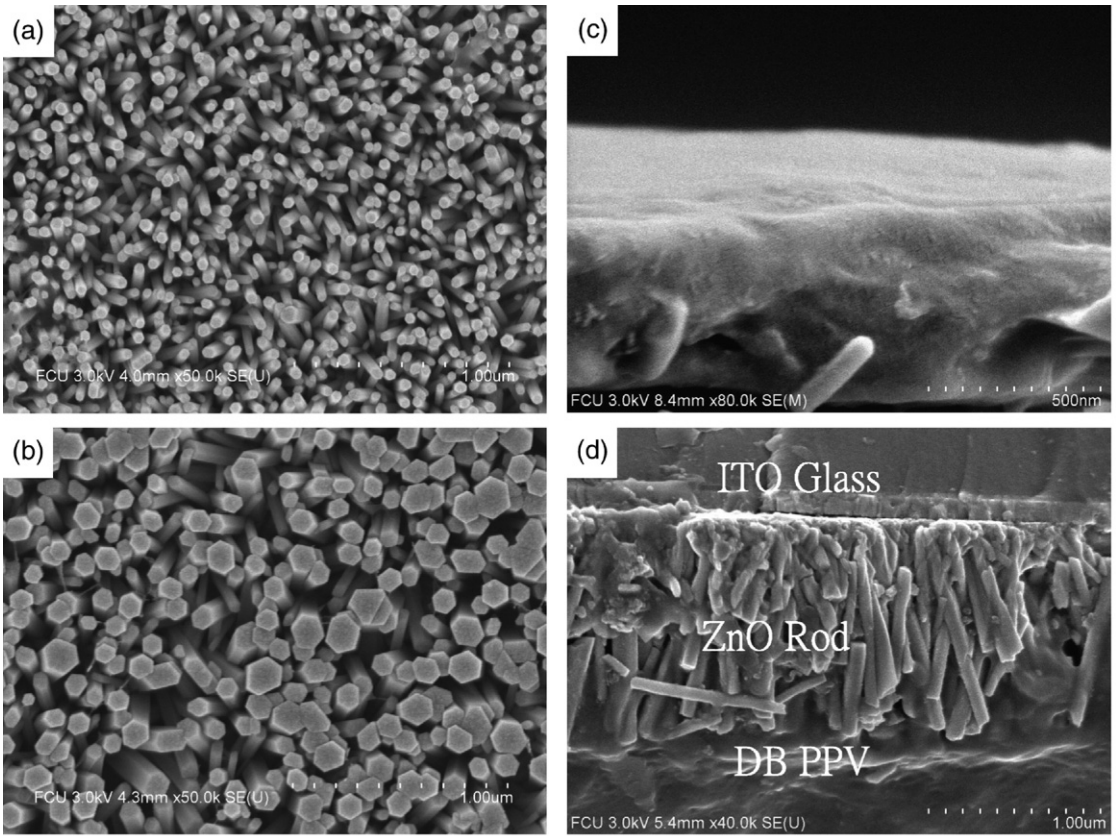

Fig. 2. FESEM images of ZnO nanorods (a) with 2 h of rod growth time (b) with 4 h of rod growth time and cross-sectional FESEM images of DB-PPV polymer intercalated into the ZnO seed layer/ZnO nanorod array structure of (c) DBZ12 and (d) DBZ14 film.

and the coverage of DB-PPV on the ZnO rod showed large influences on the photocurrent behaviors. Fig. 3 showed the in-situ differences between the photocurrent (Ip) and dark current (Id) of DBZ12 and DBZ14 films at different exposure time. Let the rise time (Tr) be the required time for photocurrent to increase from 10% to 90% of the max value. The decay time (Td) is the time for photocurrent to drop from 90% to 10%. Tr of the DBZ12 film for the first and second cycles are 60 and 35 s respectively. When the Xe light was turned off, the current decreased slowly. There was current accumulation for the DBZ12 film after repeated test cycles. On the contrary, the DBZ14 film with larger ZnO rod showed faster photocurrent response than the DBZ12 film did. Tr and Td of the DBZ14 film are 15 and 35 s respectively. There was no current accumulation for the DBZ14 film after repeated test cycles. However, the photocurrent of the DBZ14 film was lower than that of the DBZ12 film. In DBZ14 hybrid film, there were some ZnO nanorods that were not covered by the DB-PPV polymer

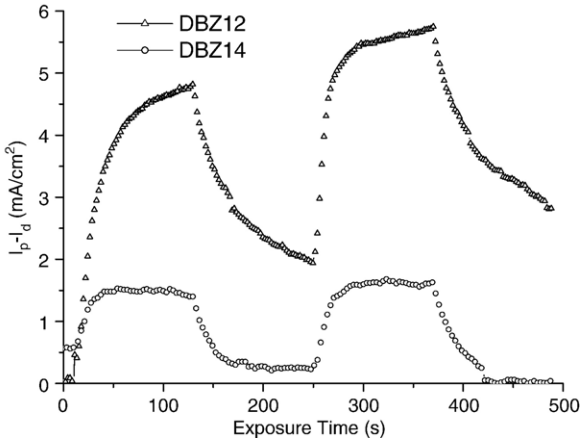

Fig. 3. In-situ difference between the photocurrent (Ip) and dark current (Id) of DBZ12 and DBZ14 films at different exposure times.

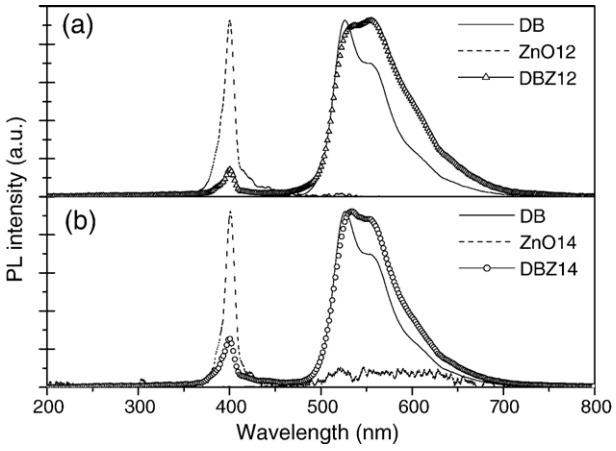

Fig. 4. PL spectra of (a) ZnO12 nanorod, DB-PPV polymer and DBZ12 hybrid film (b) ZnO14 nanorod, DB-PPV polymer and DBZ14 hybrid film.

(shown in Fig. 2(b)). The closely packed rods with almost zero inter-rod distance hindered the infiltration of polymer into the nanorod array. It may be the reason why the DBZ14 film exhibit lower photocurrent than the DBZ12 film did. The donor-ac-arraysceptor interface area (P–N junction) of the DBZ14 film will be less than that of the DBZ12 film because of poor wetting of ZnO nanorod by the DB-PPV.

Fig. 4(a) shows the photoluminescence (PL) spectrum of ZnO12 nanorods excited with 350 nm emission. The PL measurement of ZnO12 showed strong emission at 400 nm with some defect emission located between 450 and 550 nm. The emission at 500 nm has been attributed to singly ionized oxygen vacancies which arise from oxygen-deficient processing conditions such as those encountered in vapor phase growth [11] or solution-grown nanorods [12]. At the excitation of 350 nm, the emission maximal peak of DB-PPV polymer bulk film appeared at 520 nm, with a shoulder at 555 nm. The shoulder/maximum PL intensity ratio is 0.75. For the DBZ12 hybrid film, the maximum is located at 555 nm, with a shoulder at 540 nm. Incorporation of the ZnO nanorod array resulted in the enhancement of the one at 555 nm to be the maximum, and the suppression of the peak at 540 nm. The shoulder/maximum PL intensity ratio is 0.97. The PL spectrum of DBZ12 hybrid film showed a red-shift of about 17–31 nm at the right half of the peak. Since little emission in the range of 400–600 nm was observed for the ZnO12 nanorod film, the enhancement of the 555 nm component could not be attributed to the emission of ZnO12 nanorod. Similar results in the PL characteristics have been observed in composites made by PPV or its derivatives with inorganic materials [13]. The red-shift of PL may attribute to the change of the environment of the single polymer chain at the ZnO/polymer interface. PL spectral shifts depend strongly on conjugation length [14]. The observed red-shift in the emission spectrum of DBZ12 hybrid film revealed that the effective conjugation length of DB-PPV in the DBZ12 hybrid film is longer than that in the pure polymer. Because of the repulsion between the side-groups on the polymer chain, polymer chains in pure conjugated polymer film favored a relatively less planar conformation [15]. That is, polymer chains in pure conjugated polymer favored shorter conjugated length. Attaching of the polymer chains on the ZnO nanorod surface favors more planar molecular orientations, and the more planar orientations lead to an increase in effective conjugation length and a resultant of the red shift. Thus nanocomposite resulted in the enhancement of the one at 555 nm, and the suppression of the peak at 540 nm.

Fig. 4(b) shows the photoluminescence (PL) spectrum of ZnO14 nanorods excited with 350 nm emission. PL measurement of ZnO14 shows strong emission at 400 nm with some defect emission located between 500 and 650 nm. For the DBZ14 hybrid film, the maximum is located at 530 nm, with a shoulder at 555 nm. The PL spectrum of DBZ14 hybrid film also showed a red-shift at the right half of the peak.

4. Conclusions

Vertically aligned ZnO nanorods were used as electron acceptors that provided a direct and ordered path for photo-generated electrons to the collecting electrode. The number density of nanorods decreases after longer growth time. ZnO14 film with longer rod-growth time showed larger rod diameter and smaller distances between the ZnO rods than the ZnO12 analog did. Decreased distances between the rods made the structure difficult to be filled with DB-PPV polymer. ZnO nanorods that were not covered by DB-PPV were observed in the cross-sectional SEM images of the DBZ14 film. It leads to the decrease of the PN junction area and explains why the photocurrent of the DBZ12 hybrid film is larger than that of the DBZ14 hybrid film. The DBZ14 film with larger ZnO rods showed faster photocurrent response than the DBZ12 film did. After repeated test cycles, there was current accumulation for the DBZ12 film. On the contrary, no current accumulation was found for the DBZ14 film. The red shift of the photoluminescence peak suggests that filling the polymer into the ZnO rod microstructure favors more planar molecular orientations of the conjugated DB-PPV polymer and increases the effective conjugation length. Careful control of the rod alignment, inter-rod distance, rod diameters and complete coverage of the rods by the DB-PPV polymer are very important to efficient dissociation of all generated excitons, and subsequent transport of charge carriers out of the DB-PPV/ZnO nanorods hybrid film.

Acknowledgement

The authors would like to thank the financial support from the National Science Council under the contract of NSC-94-2216-E-035-020.

References

[1] W.J.E. Beek, M.M. Wienk, R.A.J. Janssen, Adv. Mater. 16 (2004) 1009.
[2] P.A. van Hal, M.M. Wienk, J.M. Kroon, W.J.H. Verhees, L.H. Sloof, W.J.H. van Gennip, P. Jonkheijm, R.A.J. Janssen, Adv. Mater. 15 (2003) 118.
[3] M.H. Huang, S. Mao, H. Feick, H. Yan, Y. Wu, H. Kind, E. Weber, R. Russo, P. Yang, Science 292 (2001) 1899.
[4] J.J. Wu, S.C. Liu, Adv. Mater. 14 (2002) 215.
[5] K. Govender, D.S. Boyle, P. O'Brien, D. Binks, D. West, D. Coleman, Adv. Mater. 14 (2002) 1221.
[6] L. Vayssieres, Adv. Mater. 15 (2003) 464.
[7] P. Ravirajan, A.M. Peiro, M.K. Nazeeruddin, M. Graetzel, D.D.C. Bradley, J.R. Durrant, J. Nelson, J. Phys. Chem., B 110 (2006) 7635.
[8] D.C. Olson, J. Piris, R.T. Collins, S.E. Shaheen, D.S. Ginley, Thin Solid Films 496 (2006) 26.
[9] K.M. Coakley, Y. Liu, M.D. McGehee, K.L. Frindell, G.D. Stucky, Adv. Funct. Mater. 13 (2003) 301.
[10] H. Miyashita, T. Satoh, T. Hirate, Superlattices Microstruct. 39 (2006) 67.
[11] K. Vanheusden, W.L. Warren, C.H. Seager, D.R. Tallant, J.A. Voigt, B.E. Gnade, J. Appl. Phys. 79 (1996) 7983.
[12] D. Wang, C. Song, J. Phys. Chem., B 109 (2005) 12697.
[13] D.F. Qi, K.R. Kwong, K. Rademacher, M.O. Wolf, J.F. Young, Nano Lett. 3 (2003) 1265.
[14] B.C. Hess, G.S. Kanner, Z. Vardeny, Phys. Rev., B 47 (1993) 1407.
[15] C.S. Cui, M. Kertesz, Phys. Rev., B 40 (1989) 9661.